Mechanism of Proton Transfer Inhibition by Cd^{2+} Binding to Bacterial Reaction Centers: Determination of the pK_A of Functionally Important Histidine Residues†

M. L. Paddock,‡ L. Sagle,‡ A. Tehrani,§ J. T. Beatty,§ G. Feher,‡ and M. Y. Okamura*,‡

Department of Physics 0319, University of California at San Diego, 9500 Gilman Drive, La Jolla, California 92093, and Department of Microbiology and Immunology, University of British Columbia, Vancouver, British Columbia, Canada V6T 1Z3

Received April 28, 2003; Revised Manuscript Received June 11, 2003

ABSTRACT: The bacterial photosynthetic reaction center (RC) uses light energy to catalyze the reduction of a bound quinone molecule Q_B to quinol Q_BH_2. In RCs from *Rhodobacter sphaeroides* the protons involved in this process come from the cytoplasm and travel through pathways that involve His-H126 and His-H128 located near the proton entry point. In this study, we measured the pH dependence from 4.5 to 8.5 of the binding of the proton transfer inhibitor Cd^{2+}, which ligates to these surface His in the RC and inhibits proton-coupled electron transfer. At pH <6, the negative slope of the logarithm of the dissociation constant, K_D, versus pH approaches 2, indicating that, upon binding of Cd^{2+}, two protons are displaced; i.e., the binding is electrostatically compensated. At pH >7, K_D becomes essentially independent of pH. A theoretical fit to the data over the entire pH range required two protons with pK_A values of 6.8 and 6.3 (±0.5). To assess the contribution of His-H126 and His-H128 to the observed pH dependence, K_D was measured in mutant RCs that lack the imidazole group of His-H126 or His-H128 (His → Ala). In both mutant RCs, K_D was approximately pH independent, showing that Cd^{2+} does not displace protons upon binding in the mutant RCs, in contrast to the native RC in which His-H126 and His-H128 are the predominant contributors to the observed pH dependence of K_D. Thus, Cd^{2+} inhibits RC function by binding to functionally important histidines.

The photosynthetic reaction center (RC)[1] from *Rhodobacter sphaeroides* is a transmembrane protein complex that catalyzes the light-induced electron and proton transfer reactions leading to reduction and protonation of a bound quinone molecule Q_B (eq 1) (*1*, *2*). Light absorbed by the

$$Q_B + 2e^- + 2H^+ + 2h\nu \xrightarrow{RC} Q_BH_2 \qquad (1)$$

RC initiates the photoionization of the primary donor, D, a bacteriochlorophyll dimer. Electrons are transferred via a bacteriochlorophyll and bacteriopheophytin to the primary quinone Q_A and then to the secondary quinone Q_B. In cell membranes, the protons required for the reduction of the quinone to quinol (eq 1) come from the cytoplasm. The Q_BH_2 leaves the RC (*3*−*6*) and is oxidized by the cytochrome bc_1 complex, thereby releasing the quinol protons into the periplasm. This creates a proton gradient across the membrane that drives ATP synthesis (*3*).

The importance of His side chains for enzyme catalysis has been well documented (*7*−*8*). In the bacterial RC, two surface His have been shown to be important for catalysis of proton transfer associated with quinol formation (eq 1) (*9*). The determination of the proton affinities (i.e., pK_A values) of the His is of fundamental importance for the proton transfer processes. In this paper, we determine the pK_A of these groups by measuring the pH dependence of the binding of the proton transfer inhibitor Cd^{2+} which has been shown to bind to these surface His (*10*). Thus, information of the thermodynamics of proton and metal binding can be obtained from the pH dependence of the dissociation constant, K_D (*11*−*13*).

The overall protonation reaction takes place in two sequential light-induced electron transfer reactions. The first light-induced reaction results in electron transfer to Q_B ($k_{AB}^{(1)}$) that is coupled to the protonation of a nearby carboxylic group Glu-L212 (Glu^- in eq 2):

$$(Q_A^-\cdot Q_B)Glu^- + H^+ \xrightarrow{k_{H^+(1)}} (Q_A^-\cdot Q_B)GluH \xrightarrow{k_{et(1)}} (Q_AQ_B^-\cdot)GluH \qquad (2)$$

(overall: $k_{AB}^{(1)}$)

where $k_{H^+(1)}$ and $k_{et(1)}$ are the rate constants for proton and electron transfer, respectively. The second light-induced reaction results in electron transfer ($k_{AB}^{(2)}$) that is coupled to the first direct protonation of the semiquinone. The mechanism of the proton-coupled electron transfer reaction

† This work was supported by the National Science Foundation (NSF Grant MCB99-82186), the National Institutes of Health (NIH Grants GM 41637 and GM 13191), and the Canadian Institutes of Health Research.

* To whom correspondence should be addressed. Phone: (858) 534-2505. Fax: (858) 822-0007. E-mail: mokamura@ucsd.edu.

‡ University of California at San Diego.

§ University of British Columbia.

[1] Abbreviations: RC, reaction center; D, primary electron donor; Q_A, neutral primary quinone electron acceptor; Q_B, neutral secondary quinone electron acceptor; Q_{10}, coenzyme Q-10 (2,3-dimethoxy-5-methyl-6-decaisoprenyl-1,4-benzoquinone); Q_BH_2, dihydroquinone (quinol); K_D, dissociation constant.

10.1021/bi0346648 CCC: $25.00
Published on Web 07/25/2003

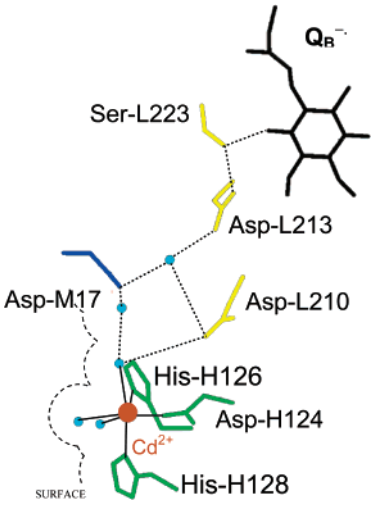

FIGURE 1: Portion of the Cd^{2+} (orange sphere) binding site in native RCs (*10*). The Cd^{2+} binds to three amino acid side chains, His-H126, His-H128, and Asp-H124, and three water molecules (blue spheres) as indicated by the solid lines. Possible hydrogen bonds connecting the surface to the Q_B binding site are indicated by dotted lines. Modified from ref *10*.

(eq 3) was shown to be a two-step process in which fast protonation precedes rate-limiting electron transfer (*14*):

$$Q_A^{-\bullet}Q_B^{-\bullet} + H^+ \xrightarrow{k_{H^+(2)}} Q_A^{-\bullet}Q_BH^{\bullet} \xrightarrow{k_{et(2)}} Q_AQ_BH^- \quad (3)$$

$k_{AB}^{(2)}$

where $k_{H^+(2)}$ and $k_{et(2)}$ are the rate constants for proton and electron transfer, respectively. Following the finding that the RC could be copurified with an externally bound Zn^{2+} (*15*), a systematic study of transition metal binding showed that Zn^{2+} and Cd^{2+} bound stoichiometrically (pH 7.8) to the RC surface. The binding of Cd^{2+} inhibited the protonation step, $k_{H^+(2)}$ (eq 3), which made proton uptake the rate-controlling step (*16*). The exact mechanism of the inhibition has been a matter of debate (*9*, *13*, *16*).

Subsequent internal proton transfer of H^+ from Glu-L212 (eq 4) leads to the formation of quinol. Note that although

$$(Q_AQ_BH^-)-GluH \rightarrow (Q_AQ_BH_2)-Glu^- \quad (4)$$

this H^+ is taken up from solution during the first electron transfer step (eq 2), it is not transferred to reduced Q_B until after the second electron transfer step (eq 3).

The protons involved in the reactions described by eqs 1−4 are taken up from the cytoplasm. Several key components of these pathways have been determined from studies of the effects of site-directed mutations in isolated RCs (*17*−*22*). Three residues (Glu-L212, Ser-L223, and Asp-L213), located near $Q_B^{-\bullet}$ (≤5 Å) were shown to be crucial (reviewed in ref *23*). The entry point of the protons was more recently identified to be near His-H126, His-H128, and Asp-H124 (Figure 1), which is the binding position of the proton transfer inhibitors Zn^{2+} and Cd^{2+} (*10*). The importance of His-H126 and His-H128 in facilitating proton transfer into the RC was subsequently established through site-directed mutagenesis (*9*).

The binding of metal ions inhibits proton transfer reactions in other membrane-bound systems such as voltage-gated proton channels (*11*) and the cytochrome bc_1 complex (*12*). Studies of the pH dependence of metal binding in these systems suggested that the metal ion ligates to a site with a pK_A near that of a His side chain (*11*, *12*). In the isolated RC, the proton transfer inhibitors Zn^{2+} and Cd^{2+} bind at the protein surface to His-H126, His-H128, and Asp-H124 (*10*). In this work, we extend previous reports on the pH dependence of metal ion binding in the RC (*13*, *24*) to obtain information on the proton affinities of the metal ion ligands, i.e., pK_a values. The determination of the pK_A of the His is important for understanding the rate and energetics of the process of proton transfer through the protein to the catalytic Q_B site. We report on the pH dependence of Cd^{2+} binding to the native RC and to mutant RCs lacking one of the side chains of the residues that form ligands to Cd^{2+}, His-H126, His-H128, and Asp-H124. We used Cd^{2+} rather than Zn^{2+} for these studies because of the greater solubility of Cd^{2+} and the tendency of the RC to precipitate at high Zn^{2+} concentrations. This allowed us to determine K_D over a pH range of ∼5 units. A preliminary account of this work has been presented (*24*).

MATERIALS AND METHODS

Reagents and Quinones. Q_{10} (2,3-dimethoxy-5-methyl-6-decaisoprenyl-1,4-benzoquinone; Sigma) was prepared in ethanol, dried under nitrogen, and solubilized in 1% LDAO (lauryldimethylamine *N*-oxide; Fluka). To maintain pH, we used a mixture of buffers consisting of 2 mM Ches [2-(*N*-cylohexylamino)ethanesulfonic acid; Sigma], Tris [tris(hydroxymethyl)aminomethane; Boehringer Mannheim], Hepes [*N*-(2-hydroxyethyl)piperazine-*N*′-2-ethanesulfonic acid; Merck], and Mes (4-morpholineethanesulfonic acid; Calbiochem). The pH was adjusted by adding NaOH or HCl. Different amounts of Cd^{2+} were added to the RC samples as follows: $CdCl_2$ was dissolved in water to make a stock solution (80 mM) whose concentration was determined (±3%) using atomic absorption, and a series of dilutions were made down to 0.1 mM. Typically, less than 10 μL was added to a 1 mL sample. All reagents were of analytical grade.

Site-Directed Mutagenesis and Preparation of Reaction Centers. The His-H126 → Ala [HA(H126)], His-H128 → Ala [HA(H128)] and Asp-H124 → Asn [DN(H124)] mutant RCs were constructed as described (*9*, *25*). RCs from *Rb. sphaeroides* R26.1 and mutant strains were purified to a ratio A^{280}/A^{800} of ≤1.3 in LDAO, and the RC concentration was determined from the A^{802} using $\epsilon = 288$ mM^{-1} cm^{-1} as described (*26*). The Q_B site was reconstituted by addition of a 3−4 times molar excess of Q_{10} in 1% LDAO, followed by dialysis against 15 mM Tris, 0.1 mM EDTA, and 0.04% dodecyl β-D-maltoside (Dojindo, Gaithersburg, MD).

Electron Transfer Measurements. Absorbance changes in response to a laser flash were measured using a setup of local design (*27*). Actinic illumination was provided by a Nd:YAG laser (Opotek, Carlsbad, CA). The pseudo-first-order rate constant $k_{AB}^{(2)}$ for electron transfer (eq 3) was determined from transient absorbance changes monitored at 450 nm following the second of two single laser flashes (λ = 800 nm). The transient spectral changes resulting from the decay of the semiquinone absorbance at 450 nm (*10*−*15*, *25*) were fitted to the sum of two exponential terms:

$$\Delta A(t) = A_F e^{-k_F t} + A_S e^{-k_S t} \quad (5)$$

where A_F and k_F are the amplitude and rate constants, respectively, for the fast component (given by the observed rate in the absence of added metal) and A_S and k_S are the amplitude and rate constant for the slow component (given by the observed rate in the presence of saturating amounts of metal). In this work we are mainly interested in the slow component. The absorbance at times longer than $1/k_{AB}^{(2)}$ is due to the absorbance change of horse heart cyt *c*, which is used as an external reductant for the light-induced oxidized RC donor, D^+. Conditions were 1 μM RCs, 30 μM horse heart cyt *c*, and 0.1% dodecyl β-D-maltoside at 21 °C.

Fittings. All fittings were performed using the nonlinear fitting algorithm Origin 6.1 (OriginLab Corp.).

Model for the Dependence of $k_{AB}^{(2)}$ on Cd^{2+} Concentration. The dependence of $k_{AB}^{(2)}$ on the concentration of Cd^{2+} (eq 4) was modeled with a simple binding curve equation (eq 6):

$$f(\mathrm{RCCd^{2+}}) = \frac{A_S}{A_S + A_F} = \frac{[Cd^{2+}]}{[Cd^{2+}] + K_D} \quad (6)$$

where $f(RCCd^{2+})$ is the fraction of the RC population with a bound Cd^{2+}, $[Cd^{2+}]$ is the concentration of free Cd^{2+}, and K_D is the dissociation constant (*7*). At the higher concentrations required to bind Cd^{2+} at lower pH, there is likely some nonspecific binding to the RC surface. This would result in a small correction of the concentration of free Cd^{2+} in solution. However, since $[RC] \ll K_D$, this correction is negligibly small.

Model for the pH Dependence of K_D. To fit the observed pH dependence of K_D, we first propose a simple model based on the known crystal structure of the Cd^{2+}-bound complex (*10*). This model entails the Cd^{2+} interacting with one titratable nitrogen atom in each of His-H126 and His-H128 as illustrated in the scheme:

$$\begin{array}{ccc} \mathrm{RC + Cd^{2+} + 2H^+} & \underset{K_D^0}{\rightleftharpoons} & \mathrm{RCCd^{2+} + 2H^+} \\ \Big\updownarrow K_A(1) & & \\ \mathrm{RCH^+ + Cd^{2+} + H^+} & & \\ \Big\updownarrow K_A(2) & & \\ \mathrm{RCH^+H^+ + Cd^{2+}} & & \end{array} \quad (7)$$

where $K_A(1)$ and $K_A(2)$ are the proton dissociation constants for each of the two titrating nitrogen atoms [having $pK_A(1)$ and $pK_A(2)$, respectively] and K_D^0 is the dissociation constant with both titrating sites deprotonated. The simplest model to fit our data includes direct competition between Cd^{2+} and H^+ for the same site. From an analysis of the reactions, we derive an expression for $K_D^{obs}(Cd^{2+})$:

$$K_D^{obs}(Cd^{2+}) = (1 + 10^{pK_A(1)-pH} + 10^{pK_A(1)-pH}10^{pK_A(2)-pH})K_D^0 \quad (8)$$

This is the same equation as used to fit similar data in other studies (*11*−*13*), except that we neglect binding of the metal ion to the singly and doubly protonated states (RCH^+Cd^{2+} or $RCH^+H^+Cd^{2+}$) which are not observed in our experiments (see Results).[2]

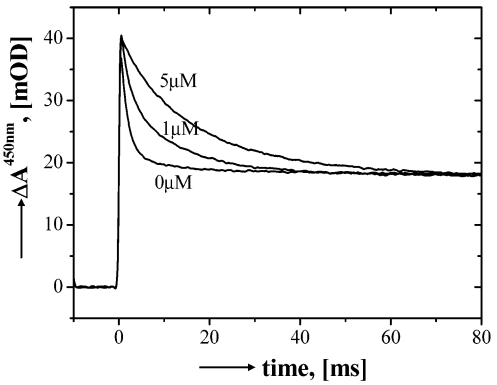

FIGURE 2: Effect of different concentrations of Cd^{2+} on the proton-coupled electron transfer $Q_A^{-\bullet}Q_B^{-\bullet} + H^+ \rightarrow Q_A^{-\bullet}Q_BH^\bullet \rightarrow Q_AQ_BH^-$ in the native RC. The observed kinetic behavior was fitted to the sum of two exponentials (eq 5). Modified from ref *16*. (Conditions: 1 μM RC, 10 mM Hepes, pH 7.5, 0.04% maltoside, and $CdCl_2$ added to the concentrations indicated.)

RESULTS

Effect of Cd^{2+} on Reaction Kinetics. The first step in obtaining a dissociation constant K_D for Cd^{2+} is to determine the fraction of RCs with a bound Cd^{2+}. For the RC, the addition of Cd^{2+} decreases the rate of the second electron transfer (eq 3). As shown previously, the rate of the overall reaction decreases as the concentration of Cd^{2+} increases (Figure 2) and is described by an increase in the fraction of RCs displaying a slow decaying component (eq 5) (*13*, *16*, *24*). It was also shown that the slower rate for the fraction of RCs with a bound Cd^{2+} is a consequence of a decrease in the rate of proton uptake (*16*) caused by Cd^{2+} binding to surface His (*10*). Thus, the observed reaction was fitted to the sum of two exponentials as shown in eq 5. From the relative amplitude of the slower decaying component (eq 6), the fraction of RCs with a bound Cd^{2+} was determined.

Determination of the Dissociation Constant K_D. From a study of the fraction of RCs with a bound Cd^{2+} as a function of the Cd^{2+} concentration, we obtained a binding curve (Figure 3). The data were fitted to a classic binding curve equation (eq 6), yielding a value for the dissociation constant K_D. The fit of the data at pH 7 yielded a value for K_D^0 of 0.4 ± 0.1 μM.

These measurements were repeated at different values of pH ranging from 4.5 to 8.5 (Figure 4). Over this range the values for k_F and k_S (eq 5) were sufficiently different (Figure 4) to allow the determination of K_D from fits to the binding data. Below pH 4.5 and above pH 8.5, K_D became difficult to determine because K_D approached the solubility limit of Cd^{2+} (lower pH) or of its hydroxide and carbonate forms (higher pH).

Fitting the Observed pH Dependence. The values for K_D at different values of pH are shown in Figure 5. We analyzed the pH dependence using eq 8 which was obtained from the

[2] The pK_A values in eq 8 are for the first and second protons, respectively. Each value is a weighted average of the intrinsic pK_A values of the imidazole groups of the two His that share the proton.

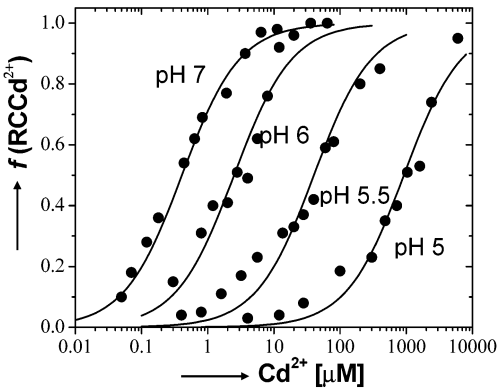

FIGURE 3: Binding curves generated from the concentration dependence of the observed kinetics at different pH values as indicated. The fraction bound was determined from the relative amplitude of the slow component (eq 6). The data were fitted to a single binding site model (eq 6) from which the value for K_D was determined. Note that the binding curves are shifted to the right with decreasing pH resulting in larger K_D values at lower pH. This is due to a competition between the metal binding and proton binding to the same sites; i.e., as the proton concentration increases at lower pH, higher concentrations of metal ions are needed to achieve 50% binding. (Conditions: same as in Figure 2.)

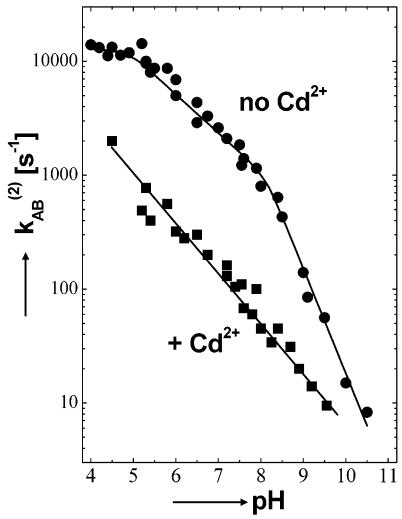

FIGURE 4: Comparison of the pH dependence of $k_{AB}^{(2)}$ for the native RC in the absence of Cd^{2+} and the presence of saturating Cd^{2+}. The rate constant in the absence of Cd^{2+} is k_F and that + Cd^{2+} is k_S (see eq 5). Note that the ratio of the rate constants is ~10 over the pH range from 4.5 to 8.5 over which the K_D data were determined and modeled. (Conditions: same as in Figure 2.)

reaction scheme of eq 7. From the fit to the data, we obtain for the three free parameters the following values:

$$K_D^0 = 0.4 \pm 0.1\ \mu\text{M}$$

$$pK_A(1) = 6.8 \pm 0.5$$

$$pK_A(2) = 6.3 \pm 0.5$$

$$pK_A(1) - pK_A(2) = 0.5 \pm 0.3 \qquad (9)$$

Attempts to fit the data to one titrating site, e.g., by eliminating the third term in eq 8, did not reproduce the steep pH dependence of K_D observed below pH 6 (see dashed line in Figure 5). In other words, the steep dependence was adequately described only by a competition between Cd^{2+}

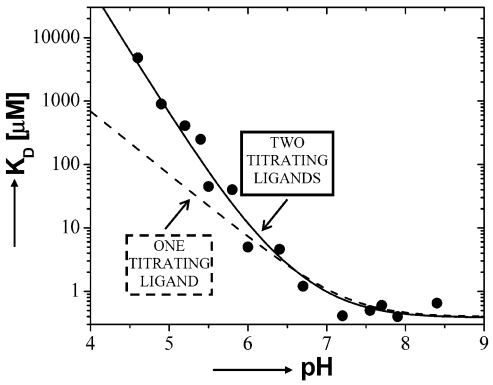

FIGURE 5: Dissociation constant of Cd^{2+}, K_D, as a function of pH for the native RC. The data were fitted to a model with one titrating metal binding ligand (dashed line, eq 8, $pK_A = 7.3$, $K_D^0 = 0.4$ μM) and two titrating metal binding ligands (solid line, eq 8, $pK_A(1) = 6.8$, $pK_A(2) = 6.3$, $K_D^0 = 0.4$ μM). Note that only the model with two titrating ligands fits the observed data at all pH values, whereas the single titrating ligand model fits only above pH 6. Above pH ~7.5 the values for K_D remain essentially unchanged as the pH is increased. (Conditions: same as in Figure 2.)

and *two* H^+. Inclusion of the singly and doubly protonated Cd^{2+}-bound states (RCH^+Cd^{2+} or $RCH^+H^+Cd^{2+}$) would result in a curve that is less pH dependent at lower pH, which is in contradiction with the data; K_D values for Cd^{2+} binding to either RCH^+ or RCH^+H^+ would be greater than 10 mM (see highest measured value for native RC at low pH in Figure 5).[3]

Effect of Site-Directed Mutations at the Cd^{2+} Binding Site on K_D. The two pK_A values determined above were assigned to specific amino acid side chains. The RC-Cd^{2+} crystal structure showed that the metal ligates to His-H126, His-H128, and Asp-H124. The pH dependence of K_D was measured in mutant RCs which carried either the His-H126 → Ala [HA(H126)] or His-H128 → Ala [HA(H128)] substitutions (Figure 6a). The overall effect of either replacement drastically changes the pH dependence of K_D: K_D^0 (K_D at high pH) is greater than in the native RC, and the pH dependence is essentially absent over the observed pH range; the perturbation of K_D^0 is greatest in the HA(H126) RC.

The pH dependence of K_D was measured in a mutant RC which carried the Asp-H124 → Asn [DN(H124)] substitution (Figure 6b). The behavior in the DN(H124) mutant RC is more similar to that of the native RC than either of the two His mutants, with a slightly greater value for K_D^0 and a pH dependence that is shifted to lower pH by ~1 unit.

DISCUSSION

The major function of the RC is to catalyze the light-induced reduction of a quinone molecule to a quinol in the Q_B site of this membrane-bound protein. This process requires the uptake of two protons from the aqueous solution (eq 1) and transports them through proton transfer pathways

[3] This is equivalent to a pK_A shift greater than 5 units upon binding of Cd^{2+} [i.e., $\log(K_D/K_D^0) > 5$]. Such a large shift cannot be explained by an electrostatically induced pK_A shift of a more central amino acid (e.g., Asp-L213) due to Cd^{2+} binding since the Coulombic interaction ($r = 14.4$ eV/$\epsilon\Delta G$) would require the distance r to be <0.5 Å even for a dielectric constant ϵ of 80 (or an even shorter distance for a lower value of ϵ). Therefore, the proton displaced upon binding of Cd^{2+} comes from one of its ligands (e.g., His-H126, His-H128, or Asp-H124) rather than from a farther amino acid.

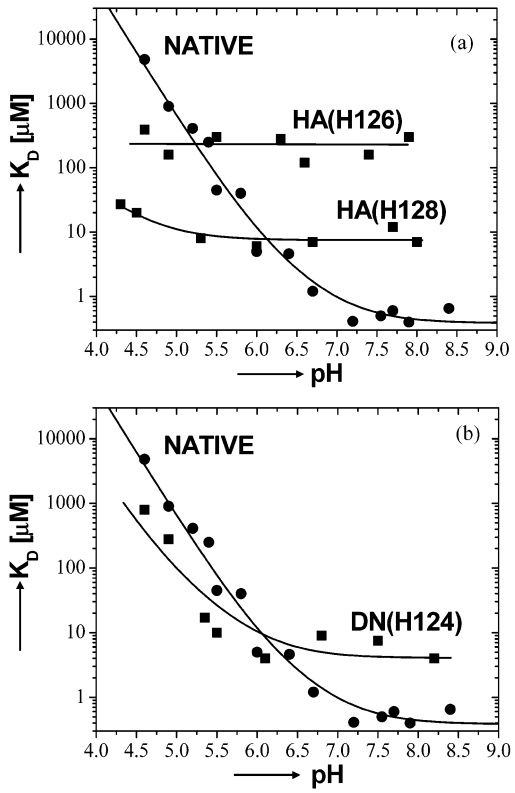

FIGURE 6: (a) Dissociation constant K_D of Cd^{2+} as a function of pH in the His-H126 → Ala [HA(H126)] and His-H128 → Ala [HA(H128)] mutant RCs (■) compared to the native RC (●). Note that the pH dependence of K_D is significantly altered in the mutant RCs lacking the imidazole group of His-H126, His-H126 → Ala [HA(H126)], or of His-H128, His-H128 → Ala [HA(H128)]. (b) Dissociation constant K_D of Cd^{2+} as a function of pH for the Asp-H124 → Asn [DN(H124)] mutant RC (■) compared to the native RC (●). Note that, in contrast to the approximate pH independence of K_D observed in the His mutant RCs, the pH dependence of K_D in the Asp-H124 → Asn RC is similar to that observed for the native RC with an ~1 unit pK_A shift to lower pH attributable to the change in charge resulting from the amino acid replacement. (Conditions: same as in Figure 2.)

that originate near the surface at two His side chains (Figure 1) (*9*, *10*, *16*). To obtain a complete understanding of the proton transfer process, a determination of the energy level of the various protonation states (i.e., pK_A values) is required. The identification of surface His at the proton pathway entry point (*9*, *10*) led us to determine their pK_A values by studying the thermodynamic competition between the proton transfer inhibitor Cd^{2+} and H^+. To prove that the His side chains contribute to the observed pH dependence, measurements were made using site-directed mutant RCs in which each His (i.e., Cd^{2+} ligand) was changed to a nontitratable side chain.

pK_A of the Surface His. The fit of the pH dependence of K_D for Cd^{2+} (Figure 5) indicates that two titrating groups, each with a pK_A value near 7, are important for the binding of Cd^{2+}. Furthermore, at low pH the slope of the logarithm of K_D versus pH approached 2, showing that two protons were released upon Cd^{2+} binding.

The apparent pK_A values of 6.8 and 6.3 for the two protons (eq 9) (approximately that of a proton bound to a His imidazole group) and the crystal structure of the metal-bound complex (Figure 1) suggested the involvement of His-H126 and His-H128. To confirm this assignment, the pH dependence of Cd^{2+} binding to a mutant RC that lacked the imidazole group of either His-H126 or His-H128 was determined (Figure 6a). The observed changes in the pH profiles of K_D show that both His-H126 and His-H128 contribute to the Cd^{2+} binding and its pH dependence in the native RC. In contrast, the replacement of Asp-H124 with Asn had relatively minor effects, in particular on the pH dependence of K_D (Figure 6b). From these results we conclude that His-H126 and His-H128 are the main contributors to the pH titration of K_D observed in the native RC.

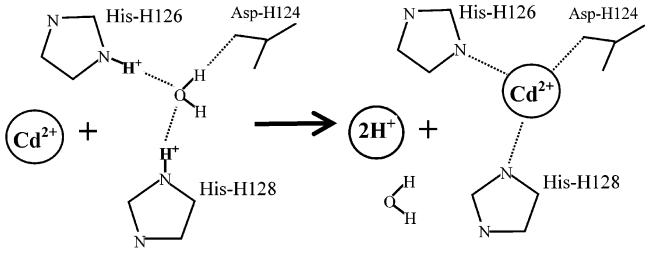

FIGURE 7: Structural schematic illustrating proton displacement by Cd^{2+} binding. Upon binding of Cd^{2+} at pH <6 two protons ($2H^+$) are released, one from His-H126 and one from His-H128. Thus, at pH < pK_A(1), pK_A(2) the binding of Cd^{2+} is electrostatically compensated by the release of two protons. Consequently, the binding of Cd^{2+} at low pH competes with the binding of two protons, which leads to the strong pH dependence of K_D (Figure 5).

Since His-H126 and His-H128 are the main contributors to the pH dependence of K_D (Figure 5), the fitted pK_A values of 6.8 and 6.3 are related to those of His-H126 and His-H128. However, we cannot assign one of these values to His-H126 and the other to His-H128 because the proton is shared between the His side chains. However, since the two pK_A values are very similar, it is reasonable to assign a pK_A value of 6.8 ± 0.5 to His-H126 and His-H128, and attribute the lower pK_A of the second proton to an electrostatic interaction between the His of ~0.5 pK_A unit; i.e., the binding of the first proton shifts the binding of the second proton by 0.5 pH unit. With this simple model, the entire pH dependence of K_D was well fitted by eq 8 (Figure 5), indicating that possible fractional proton release upon Cd^{2+} binding by other nonligand titrating sites is negligible.

The results discussed above lead to a simple picture of the binding of Cd^{2+} as shown in Figure 7. Upon binding, Cd^{2+} displaces protons that are bound to the nitrogen atoms of His-H126 and His-H128. At pH < pK_A, each His binds one H^+ that is displaced by the binding of Cd^{2+} (Figure 7). This results in the slope of ~2 for the pH dependence of log(K_D) (see pH <6 in Figure 5) and shows that Cd^{2+} binding is electrostatically compensated. At pH > pK_A, each His is unprotonated, so Cd^{2+} does not displace any H^+ upon binding and K_D becomes essentially pH independent (see pH >7.5 in Figure 5). At 6 < pH < 7, the steepness of the pH dependence of K_D varies in response to the protonation states of the His. We assume that Asp-H124 remains ionized throughout this pH range.

The changes in the values for K_D^0 of the mutant RCs compared to the native RC reflect the different binding of Cd^{2+}. The slowing down of the kinetics observed upon addition of Cd^{2+} in the mutant RCs shows that Cd^{2+} binds near the same proton entry point. However, we do not observe a pH dependence indicative of ligation to a protonated His. Therefore, in the single His mutant RCs, Cd^{2+} either

binds at a different (but nearby) site or the His is not protonated near pH 7.

The pK_A of the His at the proton transfer entry point provides an important parameter for refining the energy profile of the proton transfer process (*28*). It can be summarized as follows: the proton transfer process involves rapid reversible protonation of the His followed by proton transfer uphill by ~240 meV to an intermediate state. The energy barrier reflects the difference in pK_A between the surface His (pK_A of 6.8) and the intermediate (pK_A of ~3; *28*). This is followed by proton transfer to the terminal proton acceptor group, which is either Glu-L212 (eq 2) or $Q_B^{-\bullet}$ (eq 3).

Mechanism of Inhibition of the Bound Cd^{2+} on H^+ Transfer. The inhibition of proton uptake by the binding of metal ions (e.g., Cd^{2+}) has been previously shown (*13*, *16*, *28*, *29*). In the native RC, proton transfer $k_{H^+(2)}$ is not rate controlling for eq 3, and hence $k_{AB}^{(2)}$ was not a direct measure of k_{H^+}. Recently, using chemical rescue of a mutant RC lacking both His-H226 and His-H128, the rate constant for proton transfer was determined to be $\sim 2 \times 10^4$ s^{-1} in the pH range from 8.5 to 9.5 (*28*). Note that, in the native RC, k_{H^+} is ~20-fold greater than $k_{AB}^{(2)}$. In contrast, in the presence of a bound Cd^{2+}, proton transfer became rate controlling, and hence $k_{AB}^{(2)} = k_{H^+(2)} \sim 40$ s^{-1} (Figure 4). Hence, upon Cd^{2+} binding the observed change in $k_{AB}^{(2)}$ of ~20-fold (pH 8) is the result of an even larger ~400-fold change in k_{H^+}. Any proposed mechanism of inhibition must account for this amount of reduction.

Two possible explanations for the mechanism of inhibition of proton transfer by binding of Cd^{2+} have been discussed: (1) the metal ion binds to the His, thereby eliminating their function as proton donors/acceptors in the proton transfer step (*9*, *16*); (2) the metal ion electrostatically induces pK_A shift(s) of other functional group(s) (*13*), as a consequence of which protons are released. Although in principle both (1) and (2) could contribute to the overall decrease of proton transfer, the majority of the effect can be attributed to explanation 1; i.e., the metal ion binding inhibits the His functions as proton donors/acceptors. This conclusion is based on the similarity of the 400-fold decrease in k_{H^+} upon Cd^{2+} binding (*13*, *16*, *24*) to the 200-fold decrease in RCs in which the function of the His as proton donors was eliminated by removal of the imidazole groups of His-H126 and His-H128 by site-directed mutagenesis (His → Ala) (double His mutant) (*9*). The 2-fold difference between RCs with a bound Cd^{2+} and the double His mutant is small compared to the main 400-fold effect and may be due to an electrostatic or structural effect.

Additional results from this work provide further evidence that favors mechanism 1 over mechanism 2. Below pH 6, the binding of a Cd^{2+} ion leads to a displacement of approximately *two* protons (Figure 5), showing that there is no net change in charge upon binding of Cd^{2+}. The results also show that these protons are associated with His-H126 and His-H128. Thus, their ability to function as proton donors/acceptors is severely inhibited as required by mechanism 1. In contrast, the necessary electrostatic change required by mechanism 2 to affect pK_A values of other amino acid groups is inconsistent with the charge compensatory displacement of two protons. Furthermore, the pH dependence of the charge recombination rate constant k_{BD} ($D^+Q_AQ_B^{-\bullet} \leftrightarrow D^+Q_A^{-\bullet}Q_B \rightarrow DQ_AQ_B$) is essentially the same in RCs with and without Cd^{2+}, indicating essentially no change in the energy of the $D^+Q_B^{-\bullet}$ state upon binding of Cd^{2+} (*29*). It is difficult to attribute a 10^3-fold decrease in $k_{H^+(2)}$ to an electrostatically induced pK_A shift of internal groups (required by mechanism 2) in the absence of a change in the energy of the $D^+Q_B^{-\bullet}$ state.

Thus, the mechanism of inhibition of proton transfer by Cd^{2+} and other metals is predominantly a consequence of competing with protons for binding to His-H126 and His-H128.

Metal Binding in Other Enzymes. In many other systems, metal ion binding has been shown to inhibit function. Divalent metal ions, in particular Zn^{2+} and Cd^{2+}, have been shown to inhibit the catalytic turnover in other proton-transferring proteins, including several channels, e.g., voltage-gated proton channels (*30*), the M2 channel (*31*), and the ligand gated *N*-methyl-D-aspartate NR1/NR2A channels (*32*), and several proteins involved in proton transfer/translocation, for example, carbonic anhydrase (where it was shown that Cu^{2+} and Hg^{2+} bind to a histidine that reprotonates the Zn^{2+}–OH^-) (*33*), the cytochrome bc_1 complex (*12*, *34*), and cytochrome *c* oxidase (*35*, *36*). In the avian cytochrome bc_1 complex, two Zn^{2+} binding sites were crystallographically resolved, with the most likely inhibitory site showing ligation of the Zn^{2+} to at least one His (*34*). In cytochrome *c* oxidase Zn^{2+} was suggested to bind to surface His close to the entrance of a proton transfer pathway (*35*) as well as at the exit pathway (*36*). Inhibition of the exit pathway by Zn^{2+} and Cd^{2+} appears to compete with protons because the Zn^{2+} inhibition is 10-fold weaker at pH 6 than pH 7 (*36*). However, the metal ligands remain unidentified.

We suggest that the inhibition of catalytic activity by binding of metal ions to many different enzymes is a consequence of the common use of His as either a pH sensor or a proton donor/acceptor group (*37*). His is a likely candidate for these reactions since its pK_A is near the physiological pH ~7, and its pK_A can be "adjusted" over several pH units by the local environment (*7*, *8*). In such cases, information about the properties of functionally important residues, in particular pK_A values, can be obtained from studies of the pH dependence of metal binding affinity as reported here and elsewhere (*11*, *12*).

ACKNOWLEDGMENT

We are grateful to Edward Abresch, Charlene Chang, Shannon Foster, and Jeanette Johnson for expert technical assistance.

REFERENCES

1. Feher, G., Allen, J. P., Okamura, M. Y., and Rees, D. C. (1989) *Nature 339*, 111−116.
2. Blankenship, R. E., Madigan, M. T., and Bauer, C. E., Eds. (1995) *Anoxygenic Photosynthetic Bacteria*, Kluwer Academic Publishers, Dordrecht, The Netherlands.
3. Cramer, W. A., and Knaff, D. B. (1990) *Energy transduction in biological membranes: a textbook of bioenergetics*, Springer-Verlag, New York.
4. Crofts, A. R., and Wraight, C. A. (1983) *Biochim. Biophys. Acta 726*, 149−185.
5. McPherson, P. H., Okamura, M. Y., and Feher, G. (1990) *Biochim. Biophys. Acta 1016*, 289−292.
6. Gunner, M. (1991) *Curr. Top. Bioenerg. 16*, 319−367.

7. Fersht, A. (1999) *Structure and Mechanism in Protein Science*: *A Guide to Enzyme Catalysis and Protein Folding*, W. H. Freeman, New York, NY.
8. Creighton, T. E. (1984) *Proteins*: *Structure and Molecular Properties*, W. H. Freeman, New York, NY.
9. Ädelroth, P., Paddock, M. L., Tehrani, A., Beatty, J. T., Feher, G., and Okamura, M. Y. (2001) *Biochemistry 40*, 14538−14546.
10. Axelrod, H. L., Abresch, E. C., Paddock, M. L., Okamura, M. Y., and Feher, G. (2000) *Proc. Natl. Acad. Sci. U.S.A. 97*, 1542−1547.
11. Cherny, V. V., and DeCoursey, T. E. (1999) *J. Gen. Physiol. 114*, 819−838.
12. Link, T. A., and Vonjagow, G. (1995) *J. Biol. Chem. 270*, 25001−25006.
13. Gerencser, L., and Maroti, P. (2001) *Biochemistry 40*, 1850−1860.
14. Graige, M. S., Paddock, M. L., Bruce, J. M., Feher, G., and Okamura, M. Y. (1996) *J. Am. Chem. Soc. 118*, 9005−9016.
15. Utschig, L. M., Greenfield, S. R., Tang, J., Laible, P. D., and Thurnauer, M. C. (1997) *Biochemistry 36*, 8548−8558.
16. Paddock, M. L., Graige, M. S., Feher, G., and Okamura, M. Y. (1999) *Proc. Natl. Acad. Sci. U.S.A. 96*, 6183−6188.
17. Paddock, M. L., Rongey, S. H., Feher, G., and Okamura, M. Y. (1989) *Proc. Natl. Acad. Sci. U.S.A. 86*, 6602−6606.
18. Takahashi, E., and Wraight, C. A. (1990) *Biochim. Biophys. Acta 1020*, 107−111.
19. Takahashi, E., and Wraight, C. A. (1992) *Biochemistry 31*, 855−866.
20. Paddock, M. L., Rongey, S. H., McPherson, P. H., Juth, A., Feher, G., and Okamura, M. Y. (1994) *Biochemistry 33*, 734−745.
21. Baciou, L., and Michel, H. (1995) *Biochemistry 34*, 7967−7972.
22. Takahashi, E., and Wraight, C. A. (1996) *Proc. Natl. Acad. Sci. U.S.A. 93*, 2640−2645.
23. Okamura, M. Y., Paddock, M. L., Graige, M. S., and Feher, G. (2000) *Biochim. Biophys. Acta 1458*, 148−163.
24. Sagle, L., Paddock, M. L., Feher, G., and Okamura, M. Y. (2002) *Biophys. J. 82*, 196a.
25. Keller, S., Beatty, J. T., Paddock, M. L., Breton, J., and Leibl, W. (2001) *Biochemistry 40*, 429−439.
26. Isaacson, R. A., Lendzian, E., Abresch, E. C., Lubitz, W., and Feher, G. (1995) *Biophys. J. 69*, 311−322.
27. Kleinfeld, D., Okamura, M. Y., and Feher, G. (1984) *Biochim. Biophys. Acta 766*, 126−140.
28. Paddock, M. L., Adelroth, P., Feher, G., Okamura, M. Y., and Beatty, J. T. (2002) *Biochemistry 41*, 14716−14725.
29. Ädelroth, P., Paddock, M. L., Sagle, L. B., Feher, G., and Okamura, M. Y. (2000) *Proc. Natl. Acad. Sci. U.S.A. 97*, 13086−13091.
30. DeCoursey, T. E., and Cherny, V. V. (2000) *Biochim. Biophys. Acta 1458*, 104−119.
31. Gandhi, C. S., Shuck, K., Lear, J. D., Dieckmann, G. R., DeGrado, W. F., Lamb, R. A., and Pinto, L. H. (1999) *J. Biol. Chem. 274*, 5474−5482.
32. Low, C.-M., Zheng, F., Lyuboslavsky, P., and Traynelis, S. F. (2000) *Proc. Natl. Acad. Sci. U.S.A. 97*, 11062−11067.
33. Eriksson, E. A., Jones, T. A., and Liljas, A. (1986) in *Zinc Enzymes* (Bertini, I., Luchinat, C., Maret, M., and Zeppzauer, M., Eds.) pp 317−328, Birkhauser, Boston, MA.
34. Berry, E. A., Zhang, Z., Bellamy, H. D., and Huang, L. (2000) *Biochim. Biophys. Acta 1459*, 440−448.
35. Aagaard, A., and Brzezinski, P. (2001) *FEBS Lett. 494*, 157−160.
36. Mills, D. A., Schmidt, B., Hiser, C., Westley, E., and Ferguson-Miller, S. (2002) *J. Biol. Chem. 277*, 14894−14901.
37. DeCoursey, T. E. (2003) *Physiol. Rev. 83*, 475−579.

BI0346648